

Automatic Registration of Sea WIFS and AVHRR Imagery

Zihua Mao Delu Pan Haiqing Huang

Second Institute of Oceanography, State Oceanic Administration, Hangzhou, P. R. China

ABSTRACT An automatic approach is developed for the registration of the images from multi-temporal and multi-sensors based on coastlines derived from satellite images. One point at the coastlines is taken as one candidate point of ground control points (GCPs). The correlation-relaxation (CR) technique is employed to search the counterpart point in the second image. A decision rule is used to guarantee the accuracy of GCPs which are used to compute a polynomial equation for registering two images. The relationship between the accuracy of registration and the number of GCPs indicates that the larger number of GCPs will lead to the more accurate of image registration. The large number of accurate GCPs obtained by this method will improve the accuracy of image registration and give a chance to study new transformations of geometric rectification. The approach described in the paper can be particularly used to register images of coastal area. Examples are given for the registration of SeaWiFS and AVHRR imagery.

1. Introduction

Geometric registration of satellite data is essential in studying multi-temporal and multi-sensor images. The accuracy of registration affects the physical meanings of integrating of satellite images. Two objectives, the automatic procedure and the accuracy of registration, are mainly concerned in registration.

One of simple methods to obtain GCPs is identification of control points from the two images manually, a tedious and time-consuming task with large geometric errors. Many automatic approaches have been developed to improve the accuracy of registration and reduce time-consuming. Ventura et al. (1990) developed an automatic registration based on similarity assessment of the structures in the images and on a check of their spatial arrangement. Motrena et al. (1998) developed an automatic identification of GCPs using the auto-correlation function of an azimuthal projection around the GCP. Other automatic approaches were developed by Goshtasby et al. (1986), Cracknell and Paithoonwattanakij (1989), and Ton and Jain (1989).

Many methods for improving the accuracy of registration are also presented in literature. Cracknell and Paithoonwattanakij (1989) used chips of Landsat MSS data to improve the accuracy of rectification of AVHRR data with an accuracy of 26 percent of the pixel edge. Goshtasby et al. (1986) refined region boundaries and took the centers of gravity of closed-boundary regions as control points with subpixel accuracy.

The process of image registration is typically consisted of five steps: (1) points in the first image are selected for candidate GCPs. (2) Corresponding points in the second image are identified by a suitable point-matching technique. (3)

The accuracy of GCPs obtained from the two images is checked by a reliable decision rule. (4) The coordinates of GCPs are used to calculate the coefficients of a mapping function. (5) The mapping function is used to spatially register two images. The aim of registration procedures in this paper is to make all five steps be automatically processed.

2. Coastline as control-points

Several kinds of objects in images have been selected as GCPs, such as line intersections, line segments, gas pads, and centroid of objects, etc. For satellite images of the coastal areas, the long and continuous coastlines with obviously spatial features, satisfy all three criteria: stability, extractable, and frequency defined by Ton and Jain (1989) for an ideal control-point candidate.

2.1. Coastline extraction

Coastline, one kind of edge in the satellite image, can be extracted using edge detection technique, such as the operators of Roberts', Sobel's and Prewitt's. Roberts' algorithm is the best one to use for an image with a small amount of noise and not too slowly changing ramp edge because of its capability to detect curved edge (Peli 1982). Sobel's and Prewitt's 3×3 operators will extract thick edges and be sensitive to diagonal edges (Sethi 1982). The Rosenfeld algorithm is particularly suitable for noisy images because of its high noise immunity (Peli 1982). Suk and Hong (1982) also developed an edge extraction technique based on parallel statistical tests for noisy images. Hartley (1985) developed a Hueckel-like edge detector, a generalization of both a Gaussian gradient edge detector and of a zero crossing edge detector, for detecting multiresolution edges.

The edge detectors of Roberts', Sobel's and

prewitt's are tested on SeaWiFS and AVHRR images. The coastlines detected by Sobel's and

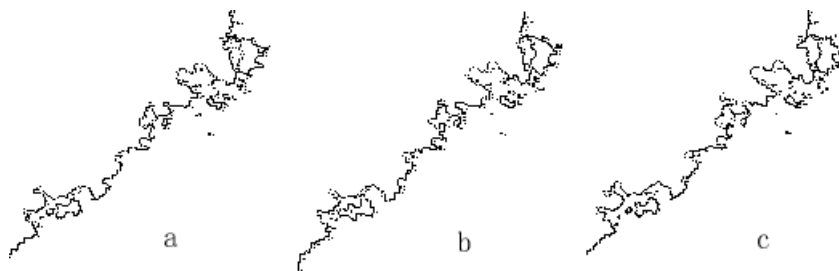


Figure 1. Coastlines extracted from a mapped SeaWiFS image of 16 August, 1998 (a), of 17 August, 1998 (b), and of 18 August, 1998 (c).



Figure 2. Coastlines extracted from a mapped AVHRR image of 16 August, 1998 (a), of 17 August, 1998 (b), and of 18 August, 1998 (c).

Prewitt's operators are similar, with two pixels width. Roberts' operator extracts coastline with one pixel width, which is suitable for extracting coastline from satellite images.

The coastline extracted from SeaWiFS images are shown in figure 1. Some preprocessings have been done before extracting coastline. SeaWiFS L1A format data was mapped by Mercator projection in the same area which is 23.95° - 25.82° N, 117.89° - 120.15° E. The size of images is 170×180 pixels. Other information except coastline was manually masked in figure 1 and 2.

The coastlines, shown in figure 2, are extracted from three sequential AVHRR images which are mapped from AVHRR 1B format data by Mercator projection with the same area and the same size as SeaWiFS. Figures 1 and 2 show that the coastlines extracted from the same satellite have similar structure, while some differences exist between coastlines derived from SeaWiFS and AVHRR images.

2.2. Geometric error analysis

Geometric mismatch between two images mapped by Mercator projection can be seen by comparison of two coastlines. Figures 3a and 3b show the integration of two coastlines and the mismatch distribution of two coastlines in eastward and northward direction. Figure 3b illustrates that the

coastline of the second image shifts right about 2.2 pixels in eastward direction. In northward direction, the upper part shifts down one pixel, the middle part do not shift, and the lower part shifts up one pixel. That means the second image is nearly two pixels smaller than the first one in northward direction.

Figure 4a is the integration of two coastlines from two AVHRR images. Figure 4b shows the mismatch distribution of two images in eastward and northward direction. The second image shifts left one pixel in eastward direction. In northward direction, the upper part of second image shifts up one pixel and the lower part shifts up 2 pixels.

Figure 5a is the integration of two coastlines from SeaWiFS and AVHRR image dated on August 16, 1998. The mismatch distribution of two images, shown in Figure 5b, is complicate and disorder. The second image shifts right about 1.4 pixels in eastward direction and shifts down about 0.0035 pixel in northward direction.

3. Searching GCPs Using Correlation-Relaxation Technique

Correlation and relaxation, used for image registration, are two of basic techniques in image processing. The correlation between the Landsat and the AVHRR image windows has been used to identify an accuracy of one-tenth of a pixel edge (Cracknell and Paithoonwattanakij 1989). A

relaxation approach is employed by Price (1986)

with feature- based symbolic description for point

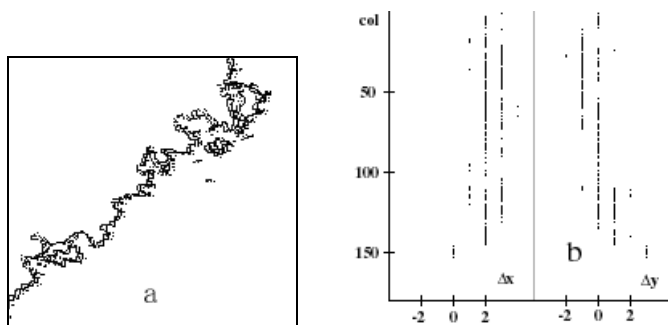


Figure 3. Integration of two coastlines extracted from two sequential SeaWiFS images (a), mismatch distribution of the two coastlines in eastward direction ($\Delta x=X_2-X_1$) and in northward direction ($\Delta y=Y_2-Y_1$), (X_1, Y_1) is the coordinate of the first SeaWiFS coastline, (X_2, Y_2) is the coordinate of the same object in the second image. Y axis is the coordinate of figure 3(a) in northward direction (b).

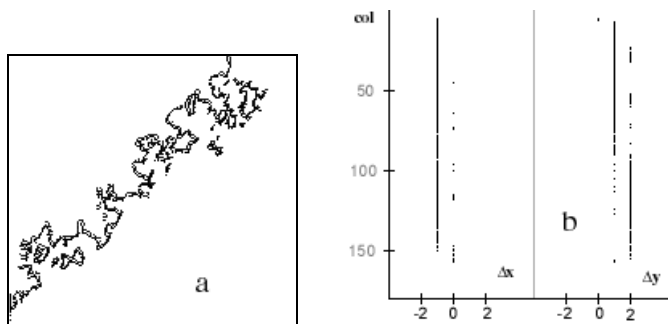


Figure 4. Integration of two coastlines extracted from two sequential AVHRR images (a), mismatch distribution of the two coastlines in eastward direction (Δx) and in northward direction (Δy) (b).

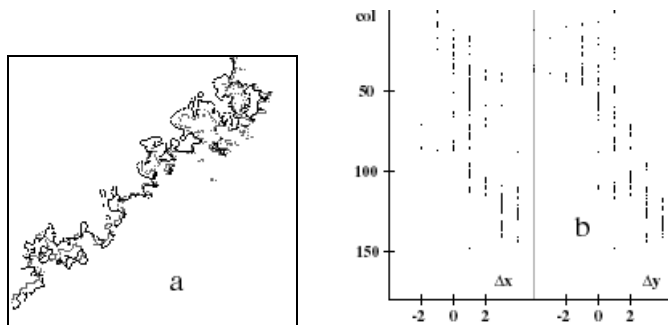


Figure 5. Integration of two coastlines extracted from SeaWiFS image and AVHRR image on the same day (a), mismatch distribution of the two coastlines in eastward direction (Δx) and in northward direction (Δy) (b).

matching. Ranade and Rosenfeld (1980) proposed a relaxation algorithm based on the distance information between points. In this paper, correlation-relaxation (CR) technique is used for point matching, which has been used to derive sea surface currents from sequential sea surface temperature (SST) images (Mao et al. 1997).

3.1 Principle of correlation-relaxation technique

One point, in the coastline of the first image, is taken as the center of a $n \times n$ matrix pattern P1

which is cut from the first image. Another matrix pattern P2 with the same size is cut from the second image within a search range S. A correlation coefficient is calculated from P1 and P2. Another coefficient can be calculated from P1 and P2 when P2 shifts one pixel position in S. A correlation coefficient matrix $[\rho]$ is produced after P2 covers all the positions in S. Some correlation-like techniques will take the point with maximum coefficient in $[\rho]$ as a matching point. Because of complexity of satellite images, especially when several points with the

same maximum values exist in $[\rho]$, the technique will lead to randomly obtain the matching points. Relaxation technique is introduced to solve the problem.

The initial probability is provided by normalized correlation coefficient matrix instead of segment type and segment size features in Ton and Jain (1989):

$$P_{ij}^0 = \rho_{ij} / \sum_r \rho_{ir} \quad (1)$$

here, ρ_{ir} is the correlation coefficient matrix.

A pair of points is taken as a vector, the relationship between two pairs can be taken as that of two vectors. The consistency strength of two vectors, where vectors refer to all candidate pairs which have bigger correlation coefficient than a threshold, is given by:

$$C = \exp(-d_1/d_0) \cdot \cos \theta \cdot \left(1 - \frac{|l_1| - |l_2|}{\max(|l_1|, |l_2|)} \right) \quad (2)$$

Therefore, the consistency strength is a function of three factors which are the distance d_1 , the angle θ and the magnitude $|l_1|, |l_2|$ of two vectors.

d_0 is an adjustable parameter. A large value of C indicates good consistency between two vectors.

The support S_{ij}^n for a given point pair is provided by the consistency strength obtained from all neighboring pairs, instead of the feature types of GCP and their distances in Ton and Jain (1989):

$$S_{ij}^n = \sum_h \sum_k C(i, j; h, k) \cdot P_{hk}^n \quad (3)$$

where, $C(i, j; h, k)$ is the consistency strength for vector l_{ij} got from vector l_{hk} . The vector l_{hk} gives a positive support to the vector l_{ij} when $C(i, j; h, k) > 0$, while it decreases the support of l_{ij} when $C(i, j; h, k) < 0$.

The normalized probability is updated iteratively by:

$$P_{ij}^{n+1} = P_{ij}^n \cdot (1 + S_{ij}^n) / \sum_r (P_{ir}^n \cdot (1 + S_{ir}^n)) \quad (4)$$

The probability of the pair changes according to the support condition from other pairs. A positive value of S_{ij}^n can increase its probability in the next iteration, while a negative one decreases its probability. A candidate point-pair will receive strong supports from other candidate point-pairs, which make them retain high probability after several iterations. The CR method uses the maximum probability to decide the candidate pair instead of maximum correlation coefficient.

3.2. Automated procedures for obtaining GCPs

Automated procedures for obtaining GCPs consist of three steps:

- (1) A point in the coastline of the first image is automatically selected as a candidate point for GCP.
- (2) The CR approach is employed to automatically search a matching point in the second image.
- (3) A decision rule automatically decides whether the point pair will be added to a set of GCPs by checking the pairs with both points locating at the coastlines.

Figure 6a shows the GCPs distribution obtained by this method from two SeaWiFS images. Points in the coastline of figure 1a are taken as candidate points in the first image. The CR approach is used to search the matching points between SeaWiFS band 8 image of 16 August, 1998 and of 17 August, 1998. The coastline of figure 1b is taken as the decision rule. Only the matching pairs, both points locating at the two coastlines, are taken as GCPs. 435 pairs of GCPs are found from two SeaWiFS images. The distribution of GCPs obtained from two AVHRR images is shown in figure 6b, which has 649 pairs of GCPs. 282 pairs of GCPs obtained from SeaWiFS image and AVHRR image are shown in figure 6c.

The results show that a large number of GCPs can be easily obtained and the accuracy of GCPs is guaranteed by the decision rule, which is very helpful in studying new geometric transformation functions and in improving the accuracy of registration.

4. Analysis of misregistration

4.1. effect of bivariate transformation

The coordinates of GCPs are used to compute a transformation function for converting the coordinates of the second image. A polynomial equation is usually used as the transformation

function, whose coefficients are calculated by the least square technique using the coordinates of GCPs. The first-order bivariate transformation can correct linear distortions with translational, rotational and scaling difference, which is used to register

images in this paper. The coefficients of 1st-order bivariate calculated from 435 pairs of GCPs of two SeaWiFS images are listed in the first row of table 1, which



Figure 6. The distribution of GCPs obtained by CR match technique from two sequential SeaWiFS images (a), that from two AVHRR images (b), and that from SeaWiFS image and AVHRR image (c). Only the points in the second image are shown.

	n	a_{00}	a_{01}	a_{10}	b_{00}	b_{01}	b_{10}
S-S	435	0.141	0.985	-0.014	0.409	0.005	0.990
A-A	649	1.119	1.000	-0.002	-1.000	0.002	0.993
S-A	282	5.810	0.971	-0.060	1.601	0.003	0.964

Table 1. Coefficients of the 1st-order bivariate transformation. S Represents SeaWiFS image, A is AVHRR image, n is the number of GCPs used to calculate coefficients which are $a_{00}, a_{01}, a_{10}, b_{00}, b_{01}, b_{10}$.

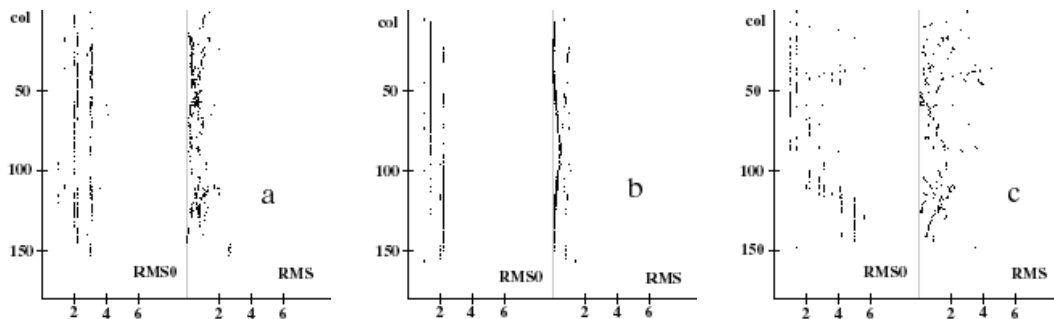


Figure 7. RMS distribution of registration of two SeaWiFS images (a), of two AVHRR images (b), and of SeaWiFS images and AVHRR image (c). RMS0 is the misregistration of two original images. RMS is the misregistration between the first image and the rectified second image.

	n	RMS0	RMS	RMS1
S-S	435	2.479	0.691	0.605
A-A	649	1.713	0.272	0.139
S-A	282	2.628	1.238	1.176

Table 2. The average of RMS0 and RMS in figure 7. RMS1 is the average of RMS after the second image resampled by the nearest neighbor interpolation.

also gives the coefficients calculated from other two sets of GCPs.

Some mismatch exists between the first image

and the new image rectified from the second image by the first-order bivariate transformation, which is quantitatively evaluated by calculating root mean

square (RMS) error. The distributions of RMS error are shown in Figure 7.

Figure 7a shows the distributions of RMSO and RMS of two SeaWiFS images. The averages of RMSO and RMS are listed in the first row of Table 2.

A new image, produced by resampling the second image using the nearest neighbor scheme, is registered to the first image with 47.4 percent of points being perfect fit together. The average of RMS1 is 0.605 pixel.

scale	S-S		A-A		S-A	
	n	RMS	n	RMS	n	RMS
1/80	5	1.869	8	0.393	3	2.676
1/40	10	0.836	16	0.347	7	1.647
1/10	43	0.706	64	0.277	28	1.414
1/4	108	0.695	162	0.279	70	1.275
1	435	0.691	649	0.272	282	1.238

Table 3. The relationship between the number of GCPs and the accuracy of geometric registration. scale is the sampling scale of GCPs. n is the number of GCPs used to calculate the coefficients of 1st-order bivariate. The average of RMS error is calculated using the total number of GCPs.

Two AVHRR images, after the second image rectified by the 1st-order bivariate transformation, can be aligned very well with 84.1 percent of points being perfect fit and the average of RMS1 is 0.139 pixel. The distributions of RMSO and RMS of two AVHRR images are shown in figure 7b.

Figure 7c shows the distribution of RMS between the SeaWiFS image and the rectified AVHRR image. Only 27.0 percent of points are perfect fit by nearest neighbor interpolation, with the average of 1.176 pixel RMS error. This big RMS is mainly caused by large location differences between the two extracted coastlines, which are caused by large difference of spectral effect from different sensors in coastal areas. The RMS of registering the whole images will be much smaller.

4.2. Effect of the Amount of Control-Points

The relationship between the number of GCPs and accuracy of registration is studied. The result is shown in Table 3. When the number of GCPs increase from 5 pairs to 435 pairs, the RMS error reduces from 1.869 pixels to 0.691 pixel, with the accuracy of registration improved by 1.178 pixels for two SeaWiFS images. The accuracy of registration has improved by 1.4 pixels for S-A images when the number of GCPs increases from 3 pairs to 282 pairs. Therefore, the more number of GCPs has the more accurate of registration. The proposed method can improve the accuracy of registration because a large number of GCPs can be easily obtained.

5. Conclusion

The main idea of automatic registration is described as following: (1) The points of the coastline extracted from the first images are taken as candidate points. (2) The CR technique is employed to search the matching-points in the second image which are checked by the coastline of the second image. (3) Only the pairs both points locating at two coastlines of the two images are taken as GCPs, which are used to calculate the coefficients of transformation. (4) The transformation is used to rectify the second image for registering with the first image. All the above procedures are supported by a software development system for automatically registering two satellite images.

Both a large number of GCPs obtained by the CR method and the accurate of GCPs guaranteed by the decision rule, are helpful to improve the accuracy of registration and give a chance to study new transformation functions.

Acknowledgements

Ocean color data used in this study were produced by the SeaWiFS Project at Goddard Space Flight Center. The data were obtained from the Goddard Distributed Active Archive Center under the auspices of the National Aeronautics and Space Administration. Use of this data is in accord with the SeaWiFS Research Data Use Terms and Conditions Agreement. The authors thank Prof. Li Yan for his valuable comments and suggestions on the first draft of the manuscript. This research was supported

by China National 863 Project (818-07-01 and 818-Q-02). The satellite data were provided by the ground station of Second Institute of Oceanography, Hangzhou, P.R. China. Their support to this research is gratefully acknowledged by the authors.

References

- Cracknell, A. P. and Paithoonwattanakij, K., 1989, Pixel and Sub-pixel accuracy in geometrical correction of AVHRR imagery. *International Journal of Remote Sensing*, 10, 661-667.
- Goshtasby, A., Stockman, G. C., and Page, C. V., 1986, A region-based approach to digital image registration with subpixel accuracy. *I.E.E.E. Transactions, Geoscience and Remote Sensing*, GE-24, 390-399.
- Hartley, R. A., 1985, Gaussian-weighted multi-resolution edge detector. *Computer Vision, Graphics and Image Processing*, 30,70-83.
- Mao, Z., Pan, D., Pan Y. and Huang, W., 1997, A new method for estimating velocity fields from satellite images. In *Recent Advances in Marine Science and Technology '96*, edited by Narendra Saxena, Pacon international, Honolulu, Hawaii, 96828, USA, 11-17.
- Motrena, P. and Rebordao, Y. M., 1998, Invariant models for ground control points in high resolution images. *International Journal of Remote Sensing*, 19, 1359-1375.
- Peli, T., 1982, A study of edge detection algorithms, *Computer, Graphics And Image Processing*, 20, 1-21.
- Price, K. E., 1986, Hierarchical matching using relaxation, *Computer Vision, Graphics and Image Processing*, 34, 66-75.
- Ranade, S. and Rosenfeld, A., 1980, Point pattern matching by relaxation. *Pattern Recognition*, 12, 269-275.
- Sethi, I. K., 1982, Edge detection using charge analogy. *Computer, Graphics and Image Processing*, 20, 185-195.
- Suk, M. and Hong, S., 1982, An edge extraction technique for noisy image. *Computer, Graphics and Image Processing*, 25, 24-45.
- Ton, J. and Jain, A. K., 1989, Registering Landsat images by point matching. *I.E.E.E. Transactions, Geoscience and Remote Sensing*, 27, 642-651.
- Ventura, A. D., Rampini, A., and Schettini, R., 1990, Image registration by recognition of corresponding structures. *I.E.E.E. Transactions, Geoscience and Remote Sensing*, 28, 305-314.